Transmission Contingency-Constrained Unit Commitment With High Penetration of Renewables via Interval Optimization

Yaowen Yu, *Student Member, IEEE*, Peter B. Luh, *Fellow, IEEE*, Eugene Litvinov, *Fellow, IEEE*, Tongxin Zheng, *Senior Member, IEEE*, Jinye Zhao, *Member, IEEE*, Feng Zhao, *Member, IEEE*, and Dane A. Schiro, *Member, IEEE*

***Abstract*—Reliability is an overriding concern for power systems that involve different types of uncertainty including contingencies and intermittent renewables. Contingency-constrained unit commitment (CCUC) satisfying the "N – 1 rule" is extremely complex, and the complexity is now compounded by the drastic increase in renewables. This paper develops a novel interval optimization approach for CCUC with N – 1 transmission contingencies and renewable generation. A large number of transmission contingencies are innovatively described by treating corresponding generation shift factors (GSFs) as uncertain parameters varying within intervals. To ensure solution robustness, bounds of GSFs and renewables in different types of constraints are captured based on interval optimization. The resulting model is a mixed-integer linear programming problem. To alleviate its conservativeness and to further reduce the problem size, ranges of GSFs are shrunk through identifying and removing redundant transmission constraints. To solve large-scale problems, Surrogate Lagrangian Relaxation and branch-and-cut (B&C) are used to simultaneously exploit separability and linearity. Numerical results demonstrate that the new approach is effective in terms of computational efficiency, solution robustness, and simulation costs.**

***Index Terms*—Interval optimization, redundant constraints, surrogate Lagrangian relaxation, transmission contingency, uncertain renewable, unit commitment.**

NOMENCLATURE

Indices and sets

c	Index of transmission contingencies, $0 \le c \le L$. $c = 0$, if the system is under the base case where no line is tripped; $c = l \neq 0$, if line *l* is tripped.
i	Index of nodes, $1 \le i \le I$.
(i, k)	Index of conventional units at node $i, 1 \le k \le K_i$.
l or *l'*	Index of transmission lines, $1 \le l \le L, 1 \le l' \le L$.
r or *r'*	Index of the maximal *(M)*, minimal *(m)*, and expected *(E)* net demand realizations.
t or *t'*	Index of time periods (hours), $1 \le t \le T$ (24), $1 \le t' \le T$ (24)
Φ^p, Φ^n	Sets of remaining interval transmission constraints in positive and negative directions, respectively.

Parameters, variables, and functions

$a_{l,c}^i$	Generation shift factor (GSF) of line *l* from node *i* under contingency *c*.
$[\underline{a}_l^i, \overline{a}_l^i]$	Interval of GSFs of line *l* from node *i* .
$C_{i,k}(p_{i,k}(t))$	Increasing convex piecewise linear generation cost function ($).
$D_i(t)$	Nodal demand at node *i* at time *t* (MW).
$\tilde{D}_i(t)$	Net nodal demand (≡ nodal demand – wind generation) at node *i* at time *t* (MW).
$\hat{D}_i(t)$	Expected value of the net nodal demand at node *i* at time *t* (MW).
$[\underline{D}_i(t), \overline{D}_i(t)]$	Interval of the net nodal demand at node *i* at time *t* (MW).
$f_l^{\max}$	Transmission capacity of line *l* (MW).
$\overline{f}_l^E(t),\ \underline{f}_l^E(t)$	Revised transmission capacities of line *l* considering the expected net demand realization at time t for positive and negative directions, respectively (MW).
$\overline{f}_l(t), \underline{f}_l(t)$	Revised transmission capacities of line *l* considering uncertain net demand at time *t* for positive and negative directions, respectively (MW).
$p_{i,k}(t)$	Generation level of unit (*i, k*) at time *t* (MW).
$p_{i,k}^r(t)$	Generation level of unit (*i, k*) at time *t* under net demand realization *r* (MW).
$p_{i,k}^{min}, p_{i,k}^{\max}$	Minimum and maximum generation limits of unit (*i, k*), respectively (MW)
$q_{i,k}(t)$	Spinning reserve of unit (*i, k*) at time *t* (MW).
$S_{i,k}$	Start-up cost of unit (*i, k*) ($/Start).
$S_{i,k}^{NL}$	No-load cost of unit (*i, k*) ($/hour).
$T_{i,k}^U,\ T_{i,k}^D$	Minimum up and down times of unit (*i, k*), respectively (hours).
$u_{i,k}(t)$	Binary start-up decision for unit (*i, k*) at time *t* .

Manuscript received January 7, 2016; revised May 15, 2016; accepted June 24, 2016. Date of publication June 28, 2016; date of current version February 16, 2017. This work was supported in part by the National Science Foundation under Grants ECCS-1028870 and ECCS-1509666, and in part by a project funded by ISO New England. A preliminary and abridged version [1] was presented in the 2015 IEEE Power and Energy Society General Meeting, Denver, Colorado, July 2015. Paper no. TPWRS-00048-2016.

Y. Yu and P. B. Luh are with the Department of Electrical and Computer Engineering, University of Connecticut, Storrs, CT 06269-4157 USA (e-mail: yaowen.yu@engineer.uconn.edu; Peter.Luh@uconn.edu).

E. Litvinov, T. Zheng, J. Zhao, F. Zhao, and D. A. Schiro are with Business Architecture and Technology, ISO New England, Holyoke, MA 01040-2841 USA (e-mail: elitvinov@iso-ne.com; tzheng@iso-ne.com; jzhao@iso-ne.com; fzhao@iso-ne.com; dschiro@iso-ne.com).

Color versions of one or more of the figures in this paper are available online at http://ieeexplore.ieee.org.

Digital Object Identifier 10.1109/TPWRS.2016.2585521

$\tilde{W}_i(t)$	Wind generation at node *i* at time *t* (MW).
$\hat{W}_i(t)$	Expected value of wind generation at node *i* at time *t* (MW).
$[\underline{W}_i(t), \overline{W}_i(t)]$	Interval of wind generation at node *i* at time *t* (MW).
$x_{i,k}(t)$	Binary UC decision for unit (*i, k*) at time *t*.
$\alpha^r(t)$	Weight of net demand realization *r* at time *t*.
$\Delta_{i,k}$	Ramp rate of unit (*i, k*) (MW/hour).
$\lambda^r(t)$	Lagrangian multiplier of the system demand constraint at time *t* under net demand realization *r* ($/MWh).
$\mu_l^r(t), \nu_l^r(t)$	Lagrangian multipliers of interval transmission constraints for positive and negative directions, respectively, at time *t* under net demand realization *r* ($/MWh).
$\sigma_i(t)$	Standard deviation of wind generation at node *i* at time *t* (MW).

I. Introduction

RELIABILITY is an overriding concern for power systems, and power engineers have been striving hard to keep the lights on under different kinds of uncertainty. One major source of uncertainty is contingencies, which are unpredicted outages of components (generators or transmission lines). To avoid cascading failures and even blackouts, the North American Electric Reliability Corporation established, among other reliability rules, the "*N* – 1 rule": for a system with *N* components, no single outage will cause violations on other components [2]. This rule has been embedded in unit commitment (UC), a critical operational process that determines the most economic set of online/offline decisions for all units one day ahead or hours ahead, resulting in "contingency-constrained unit commitment" (CCUC). Under the current practice, generator contingencies are typically managed by pre-defined reserve requirements [3]. Transmission contingencies are managed by preventive economic dispatch (ED), where ED decisions are made before contingencies are realized [3], [4]. One set of such ED decisions is guarded against the base case (under which no contingency happens) and transmission contingencies by corresponding transmission constraints in the deterministic *N* – 1 model. To avoid the complexity of directly including transmission constraints under all transmission contingencies, the "Simultaneous Feasibility Test" (SFT) is usually used [4]. The SFT determines whether a violation occurs in each post-contingency state at each hour and adds a constraint for each such violation to the next CCUC iteration. Iterations continue between CCUC and 24 SFTs (for 24 hours) until a solution with no violation is reached. Depending on the number of contingencies, this iterative process can be computationally burdensome. As a result, current practice terminates the process after a specified number of iterations and may lead to suboptimal solutions.[1]

Aside from contingencies, power systems now face new challenges associated with the uncertainty of intermittent renewables such as wind and solar [8]. Since contingencies and unexpected renewable output can occur simultaneously and cause constraint violations, a joint consideration of both factors is important. However, the resulting combinatorial complexity has limited research in this area to [9], [10] and [11]. In [9], "*N* – *k*" generator contingencies and wind uncertainty were jointly considered in UC via chance-constrained optimization. Unfortunately, transmission constraints and transmission contingencies were ignored. Authors in [10] considered transmission contingencies, generator contingencies, and wind uncertainty through stochastic programming, which minimizes the expected cost over the probability distribution of uncertainty represented by scenarios. A scenario was a combination of a contingency and a trajectory of wind realizations over 24 hours. As a result, the number of scenarios equals the product of the number of wind trajectories and the number of contingencies. After ignoring low-probability events, remaining scenarios were selected based on likelihoods proportional to their impacts on the expected cost. However, it is difficult to ensure computational efficiency while capturing low-probability but high-impact events. In [11], "*N* – 1" transmission and generator contingencies and spatially correlated nodal demand uncertainty were jointly considered for a single period through robust optimization. Although the problem was solved by using Benders decomposition and a binary expansion approach, the extension to a multi-period model would increase the computational burden significantly. Though the deterministic *N* – 1 model with the SFT is used as the current practice to manage *N* – 1 transmission contingencies, there is no publication using it for the joint consideration of contingencies and renewables to the best of our knowledge.[2]

To overcome the aforementioned complexity difficulties, this paper develops a novel interval optimization approach for the CCUC problem with preventive ED considering "*N* – 1" transmission contingencies and renewables. Section III formulates the interval CCUC problem. Instead of being analyzed one at a time, a large number of transmission contingencies are innovatively described by treating corresponding GSFs as uncertain parameters varying within intervals. In particular, under each transmission contingency, the line flow is the sum of net nodal injections weighted by corresponding GSFs. The ranges of GSFs varying among contingencies are then covered by intervals.[3] In this way, for each transmission line, we can use one single interval-based transmission constraint to represent the set of transmission constraints under all contingencies. Renewable generation is modeled by intervals and is jointly considered in the interval CCUC model in a consistent framework. To ensure solution robustness (i.e., solution feasibility under contingencies and renewable realizations), bounds of GSFs and renewable generation in different types of constraints are captured based on interval optimization [13], [14]. Since the boundary conditions of transmission contingencies and renewables are considered, there are only a few combinations. The interval model is reformulated as a mixed-integer linear programming (MILP)

[1]Another model to manage transmission contingencies (and can be used for generator contingencies) in CCUC is corrective ED. It is out of the scope of this paper, and interested readers can refer to [5]–[7].

[2]Readers interested in papers focusing on uncertain renewables without contingencies in UC can refer to the Literature Review section of [12].

[3]Although computing a large number of GSFs under transmission contingencies can be time-consuming for real-world systems, this can be implemented offline with results stored.

problem. Its conservativeness is reduced through improved interval computation.

To further reduce conservativeness and the problem size, Section IV shrinks ranges of GSFs by a pre-processing step that identifies and removes redundant transmission constraints, prior to the interval model of transmission contingencies. Such an identification method for deterministic transmission-constrained UC [15] is extended to consider uncertain renewables via interval modeling. To efficiently solve large-scale MILP problems, Section V develops a solution methodology using Surrogate Lagrangian Relaxation (SLR) [16] and branch-and-cut (B&C) [17].

Section VI tests the new approach using a simple six-bus problem, a modified IEEE Reliability Test System, and a modified IEEE 118-bus system. Optimization and simulation results demonstrate that our approach is computationally efficient and robust against transmission contingencies and renewable realizations. It also has a lower simulation cost (i.e., the expected total cost from simulation runs) than the deterministic approach.

Our approach differs from those in [12], [14], and [18]–[21] where interval optimization [13] was used to consider uncertain renewable generation or demand in UC without contingencies. While uncertain renewable generation varying within continuous ranges can be directly modeled by intervals, contingencies are often viewed as discrete events and therefore have not been looked at from an interval perspective before.

In the rest of this paper, wind generation will be used as a representative renewable resource. Although solar generation has a different diurnal pattern from wind generation, both can be modeled as intervals.

II. Interval CCUC Formulation

Section III-A describes the CCUC problem and its deterministic model, Section III-B formulates the interval optimization model considering transmission contingencies and the expected net demand, Section III-C incorporates uncertain net demand in the model, and Section III-D reduces its conservativeness through improved interval computation.

A. The CCUC Problem and the Deterministic Model

The CCUC problem is to minimize the total production cost by selecting one set of UC decisions for conventional units over the 24-hour horizon. For easy understanding of the derivation of the interval CCUC model and the redundant constraint identification method to be presented in Section IV, we start with a deterministic model, and reserves are not included in the formulation without loss of generality. The deterministic model manages transmission contingencies by multiple sets of transmission constraints and represents wind generation at each node (and the resulting net nodal demand) by its expected value. Based on [2], [22] and [23], this model can be formulated as:

$$\min \sum_{t=1}^{T}\sum_{i=1}^{I}\sum_{k=1}^{K_i}\left[u_{i,k}(t)S_{i,k}+x_{i,k}(t)S_{i,k}^{NL}+C_{i,k}(p_{i,k}^{E}(t))\right] \quad (1)$$

$$\text{s.t.} \sum_{i}\sum_{k}p_{i,k}^{E}(t)=\sum_{i}\hat{D}_i(t), \forall t, \quad (2)$$

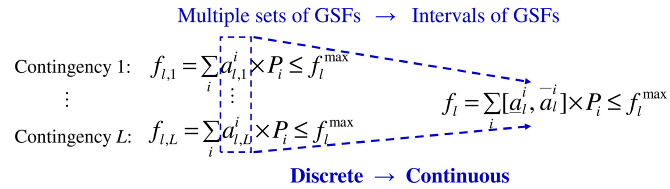

Fig. 1. Illustration of the interval contingency model. Time index t is ignored, and P_i is the net nodal injection from node i.

$$-f_l^{\max} \le \sum_i a_{l,c}^i\left(\sum_k p_{i,k}^E(t)-\hat{D}_i(t)\right) \le f_l^{\max}, \quad \forall l, \forall c \neq l, \forall t, \quad (3)$$

$$x_{i,k}(t)p_{i,k}^{\min} \le p_{i,k}^E(t) \le x_{i,k}(t)p_{i,k}^{\max}, \ \forall i, \forall k, \forall t, \quad (4)$$

$$-\Delta_{i,k} \le p_{i,k}^E(t)-p_{i,k}^E(t-1) \le \Delta_{i,k}, \ \forall i, \forall k, \forall t, \quad (5)$$

$$u_{i,k}(t) \ge x_{i,k}(t)-x_{i,k}(t-1), \ \forall i, \forall k, \forall t, \quad (6)$$

$$\sum_{t'=t-T_{i,k}^U+1}^{t} u_{i,k}(t') \le x_{i,k}(t), \ \forall i, \forall k, \forall t \in [T_{i,k}^U, \ T], \quad (7)$$

$$\sum_{t'=t-T_{i,k}^D+1}^{t} u_{i,k}(t') \le 1-x_{i,k}(t-T_{i,k}^D), \ \forall i, \forall k, \forall t \in [T_{i,k}^D, \ T]. \quad (8)$$

The objective function (1) minimizes the total UC and ED cost. System demand constraints - total conventional generation equals total *expected* net demand - are represented by (2). Transmission constraints under the base case and all "N – 1" transmission contingencies are represented by (3). Generator capacity and ramp rate constraints are given by (4) and (5), respectively. Commitment-related constraints include start-up constraints (6), minimum up time constraints (7), and minimum down time constraints (8) (deviations of (7) and (8) are in [23]).

B. Interval CCUC Formulation With Expected Net Demand

Interval optimization uses closed intervals to model uncertainties. When these intervals are captured in the constraint set, the resulting solution will be feasible for every possible uncertainty realization within them (see [13], [14]). For the CCUC problem studied here, uncertainties are present in transmission contingencies and renewable generation.

We first analyze transmission contingencies without considering wind generation uncertainties. In (3), transmission contingencies are reflected by multiple sets of GSFs (i.e., contingency-specific $a_{l,c}^i$). As each contingency is treated as a discrete event, there are L cases for line l at hour t. The total number of constraints for each direction in (3) is $T \times L^2$.

To reduce the complexity, our novel idea is to treat GSFs as uncertain parameters varying within intervals as in Fig. 1. The intervals of GSFs that capture all N – 1 transmission contingencies are determined as follows. GSFs are precalculated for all the contingencies. Then, for line l node i, the lower and upper bounds of GSFs are selected across all contingencies in (9) and (10), respectively:

$$\underline{a}_l^i = \min_{c \neq l}\{a_{l,c}^i\}, \forall l, \forall i, \quad (9)$$

$$\overline{a}_l^i = \max_{c\neq l}\{a_{l,c}^i\}, \forall l, \forall i. \tag{10}$$

These bounds establish an interval $[\underline{a}_l^i, \overline{a}_l^i]$.

The positive direction (right inequality) of (3) becomes:

$$\sum_i [\underline{a}_l^i,\ \overline{a}_l^i] \times \left(\sum_k p_{i,k}^E(t)\right) \le f_l^{\max} + \sum_i [\underline{a}_l^i,\ \overline{a}_l^i] \times \hat{D}_i(t), \forall l, \forall t. \tag{11}$$

Compared to (3), the major advantage of (11) is that only one constraint is needed to capture transmission contingencies for line *l* at hour *t*. The total number of (11) is only $T \times L$, and the reduced number of constraints is $T \times (L^2 - L)$.

To convert (11) into linear constraints, interval optimization is applied. Based on interval inequality [13], as long as the upper bound of the left-hand side (LHS) of (11) is less than or equal to the lower bound of the right-hand side (RHS), the transmission capacity will be satisfied under all contingencies. These bounds can be obtained based on interval arithmetic [24]. The bounds of the LHS are obtained as in (12), because $p_{i,k}^E(t)$ is non-negative

$$\sum_i [\underline{a}_l^i,\ \overline{a}_l^i] \times \left(\sum_k p_{i,k}^E(t)\right) = \sum_i \left[\underline{a}_l^i\left(\sum_k p_{i,k}^E(t)\right), \overline{a}_l^i\left(\sum_k p_{i,k}^E(t)\right)\right] = \left[\sum_i \underline{a}_l^i\left(\sum_k p_{i,k}^E(t)\right), \sum_i \overline{a}_l^i\left(\sum_k p_{i,k}^E(t)\right)\right], \forall l, \forall t. \tag{12}$$

As for the RHS, although the expected net nodal demand for each node *i* at each time *t* can be positive or negative, it is constant and is treated as the coefficient of the GSF intervals. The resulting interval can be obtained based on the sign of the expected net nodal demand to select corresponding bounds of GSFs, i.e.,

$$[\underline{a}_l^i,\ \overline{a}_l^i] \times \hat{D}_i(t) = \begin{cases} \left[\underline{a}_l^i\hat{D}_i(t),\ \overline{a}_l^i\hat{D}_i(t)\right], \text{ when } \hat{D}_i(t) \ge 0; \\ \left[\overline{a}_l^i\hat{D}_i(t),\ \underline{a}_l^i\hat{D}_i(t)\right], \text{ when } \hat{D}_i(t) < 0. \end{cases} \tag{13}$$

The lower bound of the RHS can thus be obtained:

$$f_l^{\max} + \sum_i [\underline{a}_l^i,\ \overline{a}_l^i] \times \hat{D}_i(t) \ge f_l^{\max} + \sum_i \min\left\{\underline{a}_l^i\hat{D}_i(t),\ \overline{a}_l^i\hat{D}_i(t)\right\} = f_l^{\max} + \sum_{i:\hat{D}_i(t)\ge 0} \underline{a}_l^i\hat{D}_i(t) + \sum_{i:\hat{D}_i(t)<0} \overline{a}_l^i\hat{D}_i(t), \forall l, \forall t. \tag{14}$$

Thus, (11) is reformulated as linear constraints:

$$\sum_i \overline{a}_l^i\left(\sum_k p_{i,k}^E(t)\right) \le f_l^{\max} + \sum_{i:\hat{D}_i(t)\ge 0} \underline{a}_l^i\hat{D}_i(t) + \sum_{i:\hat{D}_i(t)<0} \overline{a}_l^i\hat{D}_i(t), \forall l, \forall t. \tag{15}$$

In the same way, we have for the negative direction:

$$\sum_i \underline{a}_l^i\left(\sum_k p_{i,k}^E(t)\right) \ge -f_l^{\max} + \sum_{i:\hat{D}_i(t)\ge 0} \overline{a}_l^i\hat{D}_i(t) + \sum_{i:\hat{D}_i(t)<0} \underline{a}_l^i\hat{D}_i(t), \forall l, \forall t. \tag{16}$$

Other constraints (2) and (4)–(8) and the objective function (1) are not affected by transmission contingencies, and are thus unchanged. The new interval optimization model, including (1), (2), (4)–(8), (15), and (16), significantly reduces the problem size and still guarantees that all "*N* – 1" contingencies are feasible. The new model can be conservative because it ignores the dependency of GSFs on contingency (i.e., the upper or lower bounds of GSFs selected by interval arithmetic may not happen under the same contingency). This conservativeness will be reduced in Sections III-D and IV.

Note that the above interval optimization model relies on power flow equations based on GSFs to convert transmission contingencies into continuous intervals of GSFs. Other types of power flow equations, including the ones based on voltage phase angles, do not provide such intervals and therefore cannot be used to model transmission contingencies via interval optimization.

C. *Interval CCUC Formulation With Uncertain Net Demand*

This section presents how to incorporate uncertain renewables in the interval CCUC framework. Renewable generation is continuous and can thus be modeled by intervals in a consistent framework. To ensure solution robustness without much complexity, the boundary conditions of transmission contingencies and renewables are considered. The resulting conservativeness will be reduced in Section III-D.

Within the interval optimization framework, nodal wind generation is assumed to be within an interval. Wind generation at different nodes is further assumed independent of each other for simplicity [14]. The resulting net nodal demand, denoted as $\tilde{D}_i(t)$ (MW), is thus within an interval $[\underline{D}_i(t), \overline{D}_i(t)]$ with an expected value $\hat{D}_i(t)$.

1) Transmission Constraints: Substitute the expected net nodal demand with the uncertain net nodal demand in (3) and rearrange the positive direction (right inequality):

$$\sum_i a_{l,c}^i\left(\sum_k p_{i,k}(t)\right) \le f_l^{\max} + \sum_i a_{l,c}^i\tilde{D}_i(t),\ \forall l, \forall c \neq l, \forall t. \tag{17}$$

Similar to (11), the interval representation of (17) is:

$$\sum_i [\underline{a}_l^i,\ \overline{a}_l^i]\left(\sum_k p_{i,k}(t)\right) \le f_l^{\max} + \sum_i [\underline{a}_l^i,\ \overline{a}_l^i] \times [\underline{D}_i(t),\ \overline{D}_i(t)],\ \forall l, \forall t. \tag{18}$$

Its LHS is similar to that in (11), while its RHS involves the multiplication of two intervals. The lower bound of the RHS can be obtained based on traditional interval arithmetic [24]:

$$f_l^{\max} + \sum_i [\underline{a}_l^i,\ \overline{a}_l^i] \times [\underline{D}_i(t),\ \overline{D}_i(t)] \geq f_l^{\max} + \sum_i \min\{\underline{a}_l^i \underline{D}_i(t),\ \underline{a}_l^i \overline{D}_i(t),\ \overline{a}_l^i \underline{D}_i(t),\ \overline{a}_l^i \overline{D}_i(t)\},\ \forall l, \forall t. \tag{19}$$

The corresponding boundary condition of (18) can also be expressed as linear constraints:

$$\sum_i \overline{a}_l^i \left(\sum_k p_{i,k}(t)\right) \leq f_l^{\max} + \sum_i \min\{\underline{a}_l^i \underline{D}_i(t),\ \underline{a}_l^i \overline{D}_i(t),\ \overline{a}_l^i \underline{D}_i(t),\ \overline{a}_l^i \overline{D}_i(t)\},\ \forall l,\ \forall t. \tag{20}$$

The impacts of both transmission contingencies and uncertain net nodal demands on power flows are captured in (20) simultaneously without the combinatorial complexity. Constraints (20) are linear with respect to decision variables $\{p_{i,k}(t)\}$ because the bounds of GSFs and net nodal demands are input parameters, and the minimization operation can be conducted before the optimization. However, the computation of the lower bound of the RHS involves two levels of interval operations: interval multiplication (between GSF and renewable intervals) and interval addition, and may cause conservativeness through unwanted expansion of the resulting intervals. Likewise, the constraints for the negative direction are:

$$\sum_i \underline{a}_l^i \left(\sum_k p_{i,k}(t)\right) \geq -f_l^{\max} + \sum_i \max\{\underline{a}_l^i \underline{D}_i(t),\ \underline{a}_l^i \overline{D}_i(t), \overline{a}_l^i \underline{D}_i(t),\ \overline{a}_l^i \overline{D}_i(t)\},\ \forall l, \forall t. \tag{21}$$

2) System Demand Constraints: Transmission contingencies do not affect system demand, so system demand constraints [14, Eq. (20)] can be directly adopted. Since net demands at different nodes are assumed independent, we have:

$$\sum_i \sum_k p_{i,k}(t) = \sum_i [\underline{D}_i(t),\ \overline{D}_i(t)] = \left[\sum_i \underline{D}_i(t),\ \sum_i \overline{D}_i(t)\right], \forall t. \tag{22}$$

The above equation demonstrates that the boundary conditions of net system demand happen at the minimum realization *m* where all net nodal demands are at their minima, and at the maximum realization *M* where all net nodal demands at their maxima. To guarantee that generation and demand are met for any possible net nodal demand realizations, these boundary conditions are required to be satisfied:

$$\sum_i \sum_k p_{i,k}^m(t) = \sum_i \underline{D}_i(t), \forall t, \tag{23}$$

$$\sum_i \sum_k p_{i,k}^M(t) = \sum_i \overline{D}_i(t), \forall t. \tag{24}$$

Constraints (23) and (24) imply that, under the optimal UC solution, there exist two sets of ED decisions $\{p_{i,k}^m(t)\}$ and $\{p_{i,k}^M(t)\}$ that can meet *m* and *M*, respectively.

Because both system demand and transmission constraints have to be satisfied at the same time in the CCUC problem, these two sets of ED decisions $\{p_{i,k}^m(t)\}$ and $\{p_{i,k}^M(t)\}$ are also considered in LHSs of (20) and (21) based on [14].

For the same reason, generator capacity constraints (4) become:

$$x_{i,k}(t) p_{i,k}^{\min} \leq p_{i,k}^r(t) \leq x_{i,k}(t) p_{i,k}^{\max},\ \forall i, \forall k, \forall t, r = m, M. \tag{25}$$

3) Ramp Rate Constraints: The ramp rate of each unit is required to be satisfied for any self- or cross-transition between minimum (*m*) and maximum (*M*) net demand realizations in two consecutive hours, i.e.,

$$-\Delta_{i,k} \leq p_{i,k}^r(t) - p_{i,k}^{r'}(t-1) \leq \Delta_{i,k},\ \forall i, \forall k, \forall t, r = m, M, r' = m, M. \tag{26}$$

As pointed out in [12] and [21], (26) may be conservative since the cross-transitions between *m* and *M* realizations may not happen. This conservativeness can be reduced by improved ramp requirements based on the maximum possible inter-hour net demand increase and decrease [21]. In that way, the temporal correlation of the net demand (or renewable generation) can be somehow incorporated. Nevertheless, this extension is out of the scope of this paper, and (26) is still used here. In addition, the start-up and shut-down generation limits [22, eq. (11)] are considered and merged with (26) linearly.

4) The Objective Function: The goal of the optimization problem is to minimize the UC cost plus the expected ED cost of all possible wind realizations. However, the above interval constraints only contain ED decisions corresponding to the minimal and maximal realizations to reduce complexity [14]. Costs of these two extreme realizations may not reflect the costs of other possible ones. Based on [12], a weighted ED cost of minimal (*m*), maximal (*M*), and expected (*E*) realizations is used to approximate the expected ED cost with the resulting objective function:

$$\min \sum_{t=1}^{T} \sum_{i=1}^{I} \sum_{k=1}^{K_i} \left[u_{i,k}(t) S_{i,k} + x_{i,k}(t) S_{i,k}^{NL} + \alpha^E(t) C_{i,k}(p_{i,k}^E(t)) + \alpha^m(t) C_{i,k}(p_{i,k}^m(t)) + \alpha^M(t) C_{i,k}(p_{i,k}^M(t))\right]. \tag{27}$$

The constraints for the expected realization can be easily included as in Section III-B. Weights $\alpha^E(t)$, $\alpha^m(t)$, and $\alpha^M(t)$ sum up to one at each hour. They affect the optimization cost (the total cost of (27) at the optimal solution) and the simulation cost but do not affect solution robustness to uncertainty. These weights can be selected based on the system operator's preference similar to [25] since they reflect the emphases on the minimal, maximal, or expected net demand realizations. Because the majority of net nodal demand realizations are likely to happen near *E*, a guideline is that $\alpha^E(t)$ should be larger than the other weights. It is interesting to note that our objective function is a generalization of those in interval UC papers that minimize the cost of the expected realization [14], [18], [21].

The complete interval CCUC model is (2), (4)–(8), (15), (16), (20), (21), and (23)–(27) with one set of binary variables

$\{x_{i,k}(t)\}$ and $\{u_{i,k}(t)\}$, and three sets of continuous variables $\{p_{i,k}^m(t)\}$, $\{p_{i,k}^M(t)\}$, and $\{p_{i,k}^E(t)\}$. The above interval CCUC model is an MILP problem. Note that generator contingencies can be managed by pre-defined reserve requirements based on the current practice [3] through extending our model in a straightforward way.

D. Improved Interval Computation

To reduce the conservativeness of the interval CCUC model, this section focuses on improving the computing of RHS intervals in (15), (16), (20), and (21). Section IV will further alleviate the overall conservatives through shrinking the input intervals of GSFs.

Given that there are a finite number of transmission contingencies and GSF values are constant under each contingency, our idea is to pre-compute the RHS over net nodal demands under each contingency, and then select their minimum over all contingencies. For the expected realization without wind uncertainty, instead of using (14), the lower bound of the RHS of (11) is computed as:

$$f_l^{\max} + \sum_i [\underline{a}_l^i,\ \bar{a}_l^i] \times \hat{D}_i(t) \geq f_l^{\max} + \min_{c\neq l}\left(\sum_i a_{l,c}^i \hat{D}_i(t)\right) \equiv \bar{f}_l^E(t). \tag{28}$$

In the above, $\bar{f}_l^E(t)$ is the tightest lower bound of the RHS, and can be understood as a revised transmission capacity (for the positive direction) considering transmission contingencies and expected net demand. This lower bound can still be pre-computed before optimization. Thus, (15) is substituted by *interval transmission constraints*:

$$\sum_i \bar{a}_l^i \left(\sum_k p_{i,k}^E(t)\right) \leq \bar{f}_l^E(t),\ \forall l, \forall t. \tag{29}$$

In the same way, (16) is substituted by

$$\sum_i \underline{a}_l^i \left(\sum_k p_{i,k}^E(t)\right) \geq -f_l^{\max} + \max_{c\neq l}\left(\sum_i a_{l,c}^i \hat{D}_i(t)\right) \equiv \underline{f}_l^E(t),\ \forall l, \forall t. \tag{30}$$

When uncertain wind generation is considered, as net nodal demands are assumed independent, interval addition [24] is applied to compute the lower bound of the RHS of (17) (less a constant transmission capacity $f_l^{\max}$) under each contingency,

$$\min_{\tilde{D}_i(t)}\left(\sum_i a_{l,c}^i \tilde{D}_i(t)\right) = \sum_{i:a_{l,c}^i \geq 0} a_{l,c}^i \underline{D}_i(t) + \sum_{i:a_{l,c}^i < 0} a_{l,c}^i \overline{D}_i(t). \tag{31}$$

The minimum among all contingencies is then selected,

$$f_l^{\max} + \min_{c\neq l, \tilde{D}_i(t)}\left(\sum_i a_{l,c}^i \tilde{D}_i(t)\right) = f_l^{\max} + \min_{c\neq l}\left[\min_{\tilde{D}_i(t)}\left(\sum_i a_{l,c}^i \tilde{D}_i(t)\right)\right] \equiv \bar{f}_l(t), \forall l, \forall t. \tag{32}$$

In the above, $\bar{f}_l(t)$ is the tightest lower bound of the RHS, and can be understood as a revised transmission capacity (for the positive direction) considering transmission contingencies and uncertain net demand. Constraints (20) (with ED decisions $\{p_{i,k}^m(t)\}$ and $\{p_{i,k}^M(t)\}$ on the LHS) are substituted by

$$\sum_i \bar{a}_l^i \left(\sum_k p_{i,k}^r(t)\right) \leq \bar{f}_l(t),\ \forall l, \forall t, r = m, M. \tag{33}$$

Likewise, Constraints (21) are substituted by

$$\sum_i \underline{a}_l^i \left(\sum_k p_{i,k}^r(t)\right) \geq \underline{f}_l(t),\ \forall l, \forall t, r = m, M, \tag{34}$$

where $\underline{f}_l(t)$ can be pre-computed similar to (31) and (32). With (33) and (34), interval multiplication between GSF and renewable intervals is avoided, and the conservativeness of considering both contingencies and renewable at the same time is reduced.

Note that UC solutions and the resulting simulation cost are sensitive to the selection of the slack bus. Because GSFs depend on the choice of the slack bus, when the slack bus changes, GSFs change, and the derived intervals may also change. Consequently, the UC solutions and the simulation cost may also change. In this paper, a distributed slack bus is used to "average out" this dependence [26].

With improved interval computation, the interval CCUC formulation becomes (2), (4)–(8), (23)–(27), (29), (30), (33), and (34). There is still conservativeness at the LHSs of interval transmission constraints (29), (30), (33), and (34), and when considering them of different transmission lines together, because of the dependency issue of GSFs.

III. Alleviation of Conservativeness

To further alleviate the conservativeness and to further reduce the problem size, this section first identifies and removes redundant transmission constraints in the original CCUC model (1)–(8) but with uncertain renewables considered. The results of this pre-processing are then used to shrink GSF intervals considered in (29), (30), (33), and (34).

A redundant constraint identification method was developed for deterministic UC problems in [15]. An analytical estimate of the worst-case power flow along each line was obtained. If it was within the transmission capacity, the corresponding transmission constraint would be redundant, meaning that it could be removed without affecting the optimal solution.

In this section, this identification method is extended to account for uncertain wind generation. In this process, uncertain wind generation $\tilde{W}_i(t)$ cannot be treated as part of net demand. The reason is that the worst-case power flow along a line may be caused by the minimum or maximum wind realization, or other realizations within them, depending on signs of GSFs. Because the redundant constraint identification method is to find the worst-case power flow, wind generation can be modeled as intervals and be treated as conventional generation. The worst-case flow from generation in the positive direction can be estimated by solving the following MILP problem (the negative direction is similar):

$$f^*_{l,c}(t) = \max_{x_{i,k}(t),\, p_{i,k}(t),\, \tilde{W}_i(t)} \left[\sum_i a^i_{l,c} \left(\sum_k p_{i,k}(t) \right) + \sum_i a^i_{l,c} \tilde{W}_i(t) \right], \quad (35)$$

$$\text{s.t.} \sum_i \sum_k p_{i,k}(t) + \sum_i \tilde{W}_i(t) = \sum_i D_i(t), \quad (36)$$

$$-f^{\max}_{l'} \le \sum_i a^i_{l',c} \left(\sum_k p^E_{i,k}(t) + \tilde{W}_i(t) - D_i(t) \right) \le f^{\max}_{l'}, \quad \forall l' \neq l, \forall c \neq l', \quad (37)$$

$$x_{i,k}(t) p^{\min}_{i,k} \le p_{i,k}(t) \le x_{i,k}(t) p^{\max}_{i,k}, \ \forall i, \forall k, \quad (38)$$

$$\underline{W}_i(t) \le \tilde{W}_i(t) \le \overline{W}_i(t), \ \forall i. \quad (39)$$

The objective function (35) is to maximize (minimize for the negative direction) the flow of line l under contingency c at time t. Since time-coupling ramp rate and commitment-related constraints are ignored, the optimal objective value $f^*_{l,c}(t)$ is an upper bound of the actual worst-case flow.

A sufficient condition for its corresponding transmission constraint to be redundant in the CCUC problem (1)-(8) (with uncertain renewables considered) is for the maximum power flow to be less than or equal to its capacity:

$$f^*_{l,c}(t) - \sum_i a^i_{l,c} D_i(t) \le f^{\max}_l. \quad (40)$$

To avoid the computational burden of solving these MILP problems for each line, each hour, and each contingency, an analytical sufficient condition is obtained after dropping other transmission constraints (37) and integrality constraints associated with UC decisions in (38), following the development of [15, Th. 5]. Since these conditions are independent for different lines, hours, and transmission contingencies, they can be checked in parallel.

After the identification, removing redundant transmission constraints (3) does not affect results of the original CCUC model (1)–(8). However, the remaining interval transmission constraints become less conservative. More specifically, the GSF intervals $[\underline{a}^i_l, \overline{a}^i_l]$. shrink because fewer contingencies are considered. As a result, the feasibility region of decisions is larger than that of the interval CCUC problem with all of the transmission contingencies considered. The removal of redundant transmission constraints can therefore lead to a less conservative interval CCUC problem. In addition, this conservativeness alleviation technique is a pre-processing step that only shrinks GSF intervals but does not change the interval CCUC formulation as summarized at the end of Section III-D.

Another possible way to further reduce the conservativeness is to somehow consider the spatial correlation of renewable generation through affine arithmetic [27], [28] in our approach. In affine arithmetic, the interval of renewable generation at each node will be decomposed into sub-intervals associated with different sources of uncertainties based on correlations. Interval addition in (31) will then be carried out based on these sub-intervals, thereby avoiding unnecessary expansion of the resulting intervals. Affine arithmetic has been shown to provide better bounds than the standard interval arithmetic [27]. The testing with spatial correlation, however, is out of the scope of this paper.

IV. Solution Methodology

The computational process used to solve the interval CCUC problem consists of the following three steps:

1) Remove redundant transmission constraints from the original CCUC problem using the technique described in Section IV.
2) Formulate the interval CCUC problem (2), (4)–(8), (23)–(27), (29), (30), (33), and (34) as in Section III with the remaining contingencies.
3) Apply SLR [16] and B&C methods to solve the interval CCUC problem as an MILP problem.

This section focuses on Step 3.

The interval CCUC problem is formulated as an MILP problem, which is generally non-deterministic polynomial-time hard (NP-hard). Although the B&C method [17] exploits linearity, it ignores potentially beneficial problem separability so computational challenges may still arise when problems are large in scale. The purpose of our solution methodology is to find a high-quality feasible solution in a short amount of time. Therefore, the problem is decomposed into multiple unit-level subproblems that are solved by B&C. Subproblem solutions are coordinated by applying SLR [16], which has provable convergence without requiring the relaxed problem to be fully optimized and without requiring knowledge of the optimal dual value. Moreover, after solving the dual problem, feasible solutions for the original problem can be recovered using heuristics which is the best that can be expected for even the state-of-the-art branch-and-cut method in CPLEX or Gurobi. This section only includes a few necessary equations to clarify the solution methodology as an application of SLR, but does not claim SLR itself as an original contribution of this paper.

In the above interval CCUC formulation (the primal problem), units are coupled by system demand and interval transmission constraints. After relaxing these constraints, the problem becomes (constraints for the expected realization E are not included for conciseness of presentation):

$$\min \sum_{t=1}^{T} \left\{ \sum_{i=1}^{I} \sum_{k=1}^{K_i} \left[u_{i,k}(t) S_{i,k} + x_{i,k}(t) S^{NL}_{i,k} + \sum_r \alpha^r(t) \times C_{i,k}(p^r_{i,k}(t)) \right] \right\} + \lambda^m(t) \left[\sum_i \underline{D}_i(t) - \sum_i \sum_k p^m_{i,k}(t) \right] + \lambda^M(t) \left[\sum_i \overline{D}_i(t) - \sum_i \sum_k p^M_{i,k}(t) \right] + \sum_{(l,t)\in\Phi^p} \sum_{r\in\{m,M\}} \mu^r_l(t) \times \left[\sum_i \overline{a}^i_l(t) \left(\sum_k p^r_{i,k}(t) \right) - \overline{f}_l(t) \right] + \sum_{(l,t)\in\Phi^n} \sum_{r\in\{m,M\}} \nu^r_l(t) \left[\underline{f}_l(t) - \sum_i \underline{a}^i_l(t) (\sum_k p^r_{i,k}(t)) \right], \quad (41)$$

s.t. Unit-level constraints: (6)–(8), (25), and (26).

This relaxed problem can be decomposed into unit-level subproblems. For unit *k*, its subproblem is

$$\begin{aligned}\min L_k = \min\Bigg\{&\sum_{t=1}^{T}\Bigg[u_{i,k}(t)S_{i,k} + x_{i,k}(t)S_{i,k}^{NL}\\&+\sum_r \alpha^r(t)C_{i,k}(p_{i,k}^r(t))\\&-\lambda^m(t)p_{i,k}^m(t) - \lambda^M(t)p_{i,k}^M(t)\Bigg]\\&+\sum_{(l,t)\in\Phi^p}\sum_{r\in\{m,M\}}\mu_l^r(t)\bar{a}_l^i(t)p_{i,k}^r(t)\\&-\sum_{(l,t)\in\Phi^n}\sum_{r\in\{m,M\}}\nu_l^r(t)\underline{a}_l^i(t)p_{i,k}^r(t)\Bigg\}, \end{aligned}\tag{42}$$

s.t. Unit-level constraints: (6)-(8), (25), and (26) for unit *k*.

These subproblems are MILP problems that can be proven not NP-hard, and can be efficiently solved by using B&C. The optimal Lagrangian of subproblem *k*, for given dual variables, is denoted by $L_k^*(\lambda^r(t), \mu_l^r(t), \nu_l^r(t))$.

To coordinate subproblem solutions, the Lagrangian is maximized in an upper-level dual problem:

$$\begin{aligned}\max_{\lambda^r(t),\mu_l^r(t),\nu_l^r(t)}\Bigg\{&\sum_{i=1}^{I}\sum_{k=1}^{K_i}L_k^*(\lambda^r(t),\mu_l^r(t),\nu_l^r(t))\\&+\sum_{t=1}^{T}\left[\lambda^m(t)\left(\sum_i \underline{D}_i(t)\right)+\lambda^M(t)\left(\sum_i \overline{D}_i(t)\right)\right]\\&-\sum_{(l,t)\in\Phi^p}\sum_{r\in\{m,M\}}\mu_l^r(t)\overline{f}_l(t)+\sum_{(l,t)\in\Phi^n}\sum_{r\in\{m,M\}}\nu_l^r(t)\underline{f}_l(t)\Bigg\}.\end{aligned}\tag{43}$$

To efficiently solve the dual problem, SLR is used to update multiplier values. Since SLR does not require solving all subproblems to update multipliers for separable problems, at each iteration, one group of subproblems is solved and the optimal multipliers are updated based on [16].

After solving the dual problem, feasible solutions for the primal problem can be recovered using heuristics. One possible way solves a smaller CCUC problem by fixing online UC decisions for relatively cheap units (based on full load average costs) and offline UC decisions for expensive ones.

The combined SLR and B&C method is illustrated in Fig. 2.

V. Numerical Results

Three problems are tested to demonstrate properties of the interval CCUC approach. In Example 1, a simple six-bus problem is tested to demonstrate solution robustness of the interval CCUC model against transmission contingencies and examine its conservativeness. In Example 2, a modified IEEE Reliability Test System with six wind farms is tested to compare the new approach with a deterministic approach. The benefits of redundant constraint removal are also exhibited. In Example 3,

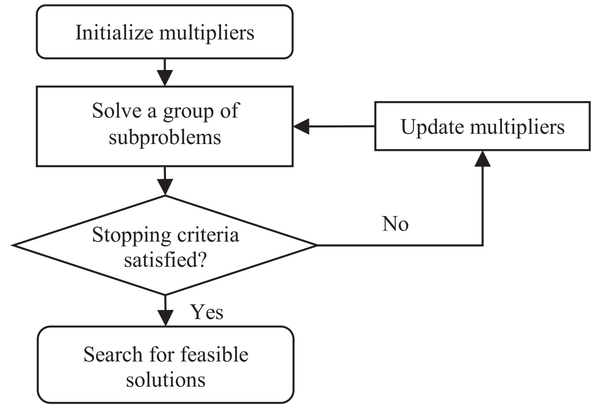

Fig. 2. Flowchart of the combined SLR and B&C method.

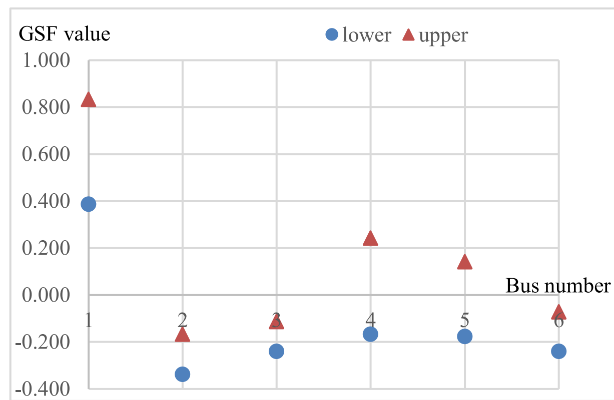

Fig. 3. GSF intervals of Line 1 at six buses of Case 1 in Example 1.

a modified IEEE 118-bus system with ten wind farms is tested to demonstrate the computational efficiency of SLR. Examples 1 and 2 are tested on a PC laptop with an Intel i7-2820QM 2.30GHz CPU (4 cores and 8 threads) and 8GB memory, while Example 3 on a PC laptop with an Intel i7-6920HQ 2.90GHz CPU (4 cores and 8 threads) and 32GB memory. Optimization and simulation of all examples are conducted using CPLEX 12.5.1.0 with OPL.[4]

Example 1: The six-bus test problem from [7] is solved for a one-hour period. Uncertain renewable generation is not considered, and the quadratic cost function of each generator is approximated by a single bid block and a no-load cost.

Case 1: To illustrate the interval CCUC model, intervals of GSFs of Line 1 at six buses are plotted in Fig. 3. These GSF intervals, consisting of lower and upper bounds, are used to capture the base case and 8 contingency cases in transmission constraints in the interval CCUC model.

The interval CCUC model is solved using pure B&C without redundant constraint identification. Since the interval CCUC model is a simplified model, simulation is conducted to evaluate its UC solution. In simulation, the optimal UC solution is used as input and the $N-1$ contingency-constrained ED problem is solved. As a benchmark, the original CCUC model (1)–(8) is also tested. The original CCUC model does not need additional

[4]Testing data and results are available at http://www.engr.uconn.edu/msl/J1_IEEE.htm.

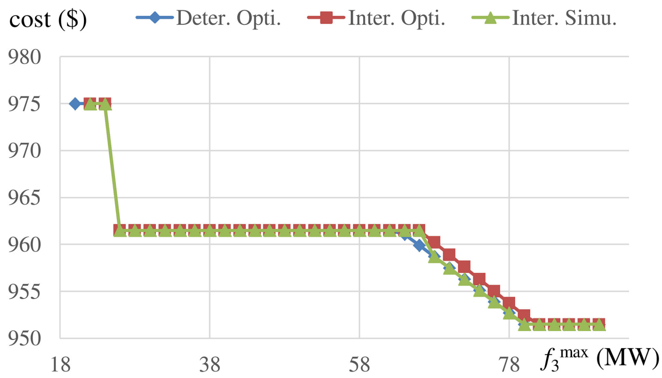

Fig. 4. Optimization and simulation results of Case 1 in Example 1.

simulation, since $N-1$ contingency-constrained ED is included within the model, and its optimization and simulation costs are thus the same.

To examine the impact of transmission limits on costs, the problem is solved with $f_3^{\max}$ increasing from 18 MW to 90 MW in 2 MW increments. Optimization and simulation costs are summarized in Fig. 4.

Both models are infeasible when $f_3^{\max}$ is 18 MW. The original model becomes feasible when $f_3^{\max}$ is 20 MW, and the interval model does when $f_3^{\max}$ is 22 MW. When both models are feasible, the optimization cost of the interval model is higher than or equal to that of the original model, since the interval model can be more conservative. The largest percentage difference between these two costs is 0.17%.

The simulation process of the interval model is feasible as long as its optimization process is feasible, indicating that its solution is robust against contingencies. Moreover, its optimization cost is at least its corresponding simulation cost (i.e., the optimal UC cost plus the simulated ED cost), showing that the former can serve as the upper bound of the latter when only contingencies are considered. The simulation cost of the interval model equals that of the original model where their UC solutions turn out to be the same, except when $f_3^{\max}$ is 64 or 66 MW. This demonstrates that the conservativeness of the interval model is not high in this case.

Case 2: To demonstrate the sensitivity of our interval CCUC model to the selection of the slack bus, optimization is performed with different slack buses, and simulation is then conducted with UC solutions from optimization. Transmission capacity $f_3^{\max}$ is fixed at 60 MW. Results are summarized in Table I (the time index t is omitted since only one period is considered in this example).

The optimization cost changes when the slack bus changes, and it appears that when the distributed slack bus is selected, the optimization cost is the lowest. The reason is that the power flow from demand, $\sum_i a_{l,c}^i \hat{D}_i(t)$, at the RHSs of (29) (obtained in (28)) and (30) is always zero with the distributed slack bus. The resulting interval of the power flow from demand, $[\min_{c\neq l}(\sum_i a_{l,c}^i \hat{D}_i(t)),\ \max_{c\neq l}(\sum_i a_{l,c}^i \hat{D}_i(t))]$, is the narrowest as a point 0. This demonstrates that the distributed slack bus is the least conservative among different slack bus choices.

TABLE I
OPTIMIZATION AND SIMULATION RESULTS OF CASE 2 IN EXAMPLE 1

Slack	Opti. ($)	$x_{1,1}$	$x_{3,1}$	$x_{5,1}$	Simu. ($)
1	968.28	1	1	0	963.50
2	969.66	1	1	0	963.50
3	961.50	1	0	0	961.50
4	967.15	1	1	0	963.50
5	961.50	1	0	0	961.50
6	961.50	1	0	0	961.50
7	961.50	1	0	0	961.50
8	961.50	1	0	0	961.50
Dist.	961.50	1	0	0	961.50

UC decisions and the resulting simulation cost also change when the slack bus changes, but are less sensitive to the selection of the slack bus than the optimization cost. The simulation cost is also the lowest when the distributed slack bus is selected, since this selection is the least conservative.

Example 2: Consider the IEEE RTS as modified in [1]. There are 38 transmission lines with reactance values, normal capacities, and long-term emergency (LTE) capacities for transmission contingencies [29]. To avoid islanding or infeasibility when the line from Bus 7 to Bus 8 is tripped, the line between those buses is replaced by two parallel lines, each with a reactance of 0.123 p.u., a normal capacity of 175 MW, and an LTE capacity of 208 MW. There are 24 conventional units, two must-run nuclear units, and six base-load hydroelectric units.

Six 110 MW wind farms are added to the model. Wind generation of each wind farm in each hour (normalized by capacity) is assumed to follow a normal distribution truncated at two standard deviations and the physical limits [0, 1]. Its expected values for 24 hours are based on the day-ahead forecasts of a wind site on August 1, 2006 from [30]. Its standard deviation, denoted as $\sigma_i(t)$ for node i at hour t, is assumed to depend on the corresponding expected value [31]:

$$\sigma_i(t) = 0.02 + 0.2\hat{W}_i(t), \forall i, \forall t. \tag{44}$$

Case 1: Our approach is compared with the deterministic approach. Demand data from Tuesday of Week 28, a Summer Weekday, is used [29]. The wind penetration ($\equiv$ total expected wind generation / total demand $\times$ 100%) is 18.9%.

The analytical sufficient condition is checked in serial using MATLAB R2014a and uses the CPU time of 2.25 seconds. The original number of transmission constraints is 219,024 [$= 39^2 \times 24 \times 2$ (positive and negative directions) $\times$ 3 (m, M, and E realizations)]. The number of interval transmission constraints after the removal of the redundant constraints is 705, demonstrating a significant reduction of the model size.

The interval CCUC model is solved using pure B&C with and without the redundant constraint identification. In optimization, the weights in (27) are $\alpha^E(t) = 0.8$ and $\alpha^m(t) = \alpha^M(t) = 0.1$.

For benchmarking, the deterministic approach (1)–(8) is also tested. To provide a fair comparison with our interval optimization approach, uncertain wind generation is managed by spinning reserves [32]. The system spinning reserve requirements are set as the sum of two standard deviations over all

TABLE II
OPTIMIZATION AND SIMULATION RESULTS OF EXAMPLE 2

	Approach	Deter.	Inter. w/o iden.	Inter. w/ iden.
Optimization	Total cost (k$)	236.03	298.18	246.87
	CPU time (s)	5.88	21.98	4.01
Simulation	E(Total cost) (k$)	254.26	275.36	245.84
	STD(Total cost) (k$)	1.91	1.38	1.47
	99.7% confidence interval of E(Total cost) (k$)	[254.08, 254.44]	[275.23, 275.49]	[245.70, 245.98]
	E(Load shed penalty) (k$)	0.20	0	0
	E(Wind curtailed penalty) (k$)	0	0	0
	# of runs incurring penalties	32	0	0

wind farms, i.e.,

$$\sum_i \sum_k q_{i,k}(t) \geq \sum_i 2\sigma_i(t), \forall t. \tag{45}$$

The spinning reserve of each unit plus its generation level should be within its capacity, i.e.,

$$x_{i,k}(t)p_{i,k}^{\min} \leq p_{i,k}^E(t)+q_{i,k}(t) \leq x_{i,k}(t)p_{i,k}^{\max}, \forall i, \forall k, \forall t. \tag{46}$$

The optimization for each approach is terminated at a relative MIP gap 0.01%.

To evaluate the solution of each approach, 1,000 Monte Carlo simulation runs are conducted. 1,000 wind scenarios are sampled from truncated normal distributions, i.e., one scenario for each run. In each run, UC decisions are fixed at the solution obtained from optimization, and a 24-hour deterministic $N-1$ contingency-constrained ED problem is solved. Each such ED problem considers all possible $N-1$ transmission contingencies in transmission constraints similar to (3) based on the "$N-1$ rule." To address possible infeasibility issues, wind generation can be curtailed at a penalty cost of $150/MWh,[5] while load can be shed at a penalty cost of $5,000/MWh. Note that wind curtailment or load shedding is not allowed for all approaches in optimization to demonstrate the solution robustness of our approach (i.e., as long as there is one feasible UC solution obtained from optimization, it will be feasible against all $N-1$ transmission contingencies and possible wind realizations). If the problem becomes infeasible in other systems, load shedding and wind curtailment can be considered similar to conventional generation (wind curtailment as negative generation) as decision variables in our interval optimization approach with penalty costs.

Results are summarized in Table II. With the redundant constraint identification, the optimization cost of the interval CCUC model decreases from $298.18k to $246.87k, and the simulation cost decreases by 12.01% from $275.36k to $245.84k. This demonstrates that the model and the resulting UC solution are less conservative, after redundant constraints are removed.

[5]This penalty cost provides priority for wind generation to be dispatched. The bid floor of wind generation at the California ISO is −$150/MWh [33], i.e., 1 MWh of wind generation is can at most reduce $150 from the total cost. Correspondingly, 1 MWh of wind curtailment is penalized at $150.

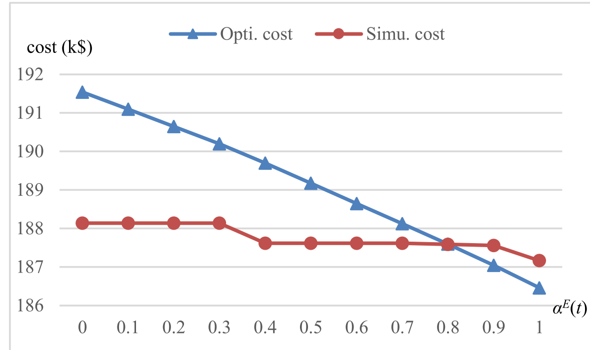

Fig. 5. Sensitivity of optimization and simulation costs with respect to $\alpha^E(t)$.

Although our approach with the identification still has a higher optimization cost than the $236.03k from the deterministic approach, our approach has a 3.42% lower simulation cost. The interval approach avoids wind curtailment and load shedding in all simulation runs, demonstrating its solution robustness. The deterministic approach, on the other hand, requires load shedding in 32 out of 1,000 scenarios. This indicates that the deterministic approach, even with spinning reserves, cannot guarantee solution robust against all possible wind realizations.

Case 2: Different choices of weights in the objective function (22) of the interval CCUC model are tested with the redundant constraint identification. Demand data from Tuesday of Week 31, a Summer Weekday, are used [29]. The wind penetration is 21.4%.

The weight $\alpha^E(t)$ is changed from 0 to 1 at a step of 0.1. Since the truncated normal distributions assumed for wind generation are symmetric, $\alpha^m(t)$ and $\alpha^M(t)$ are chosen to be the same for simplicity. For example, when $\alpha^E(t) = 0.8$, $\alpha^m(t) = \alpha^M(t) = 0.1$. Optimization and simulation results are summarized in Fig. 5.

The optimization cost decreases as $\alpha^E(t)$ increases, indicating that the larger $\alpha^E(t)$ moves the optimization cost closer to *E* realization, and *M* realization (more expensive with higher net demand) affects the cost more than *m*. The simulation cost also decreases but more slowly, and does not change when $\alpha^E(t)$ is from 0 to 0.3, or from 0.4 to 0.7. This is because the UC solutions do not change in these ranges, although the optimal cost changes due to the weight variations in the objective function. This demonstrates that UC solutions are not very sensitive to these weights. To reflect the modeling accuracy, the absolute percentage error (APE) between optimization and simulation costs is calculated. The highest APE is 1.81% when $\alpha^E(t) = 0$, while the lowest APE turns out to be 0.00% when $\alpha^E(t) = 0.8$. The APE is below 1% when $\alpha^E(t)$ is from 0.5 to 1.

In addition, two extreme cases are also tested. When $\alpha^m(t) = 1$ (and other weights are zero), the optimization cost is $156.14k, the simulation cost $189.27, and the APE 17.50%. When $\alpha^m(t) = 1$, the optimization cost is $225.53k, the simulation cost $189.57k, and the APE 18.97%. The above results demonstrate that considering *E* realization in the objective function (13) with a relatively high weight provides an accurate approximation of the expected cost of all wind realizations. Moreover, no matter how these weights change, UC solutions are always feasible against possible renewable realizations and

TABLE III
OPTIMIZATION AND SIMULATION RESULTS OF EXAMPLE 3[6]

	Model Method	Deter. Pure B&C	Inter. w/ iden. Pure B&C	 SLR+B&C
Optimization	Total cost (k$)	797.48	834.26	834.88
	CPU time	2min14 s	58 s	56 s
	CPU time/iteration	–	–	2.80 s
	CPU time/group	–	–	0.47 s
Simulation	E(Total cost) (k$)	827.03	821.68	819.46
	STD(Total cost) (k$)	8.06	2.40	2.39
	99.7% confidence interval of E(Total cost) (k$)	[826.26, 827.79]	[821.45, 821.91]	[819.23, 819.69]
	E(Load shed penalty) (k$)	0	0	0
	E(Wind curtailed penalty) (k$)	13.49	0	0
	# of runs incurring penalties	974	0	0

contingencies, since the ranges of uncertainty are captured in constraints.

Example 3: The IEEE 118-bus system with ten additional wind farms is solved. In this model, there are 54 conventional units, 186 transmission lines, and 91 demand centers with a peak system demand of 3733.07 MW [34]. Each additional wind farm has a capacity of 100 MW, and the treatment of its generation is the same as in Example 2. The wind penetration is 17.0%. To avoid islanding or infeasibility, nine lines are added and capacities of four lines are increased, similar to [7]. The LTE capacity of each line is assumed to be 1.2 times its normal capacity.

Similar to Case 1 of Example 2, our interval CCUC model with the redundant constraint identification is compared with the deterministic model (1)–(8), (45) and (46). Both models are solved by using the pure B&C method, with a relative MIP gap 0.5% as the stopping criterion. 1,000 Monte Carlo simulation runs are then conducted to evaluate the solution of each model. The results are summarized in the first two columns of Table III.

The deterministic model takes 2 minutes and 14 seconds to solve by using pure B&C, while our interval CCUC model takes 58 seconds. This implies that the new model with redundant constraint identification is more computationally efficient than the deterministic model. Moreover, the deterministic approach incurs wind curtailment in 974 out of 1,000 scenarios. The interval model, in contrast, avoids wind curtailment and load shedding in all simulation runs. This further demonstrates the solution robustness of our interval model, in addition to results in Case 1 of Example 2.

Furthermore, our model is also solved by using the combined SLR and B&C method. In the combined method, the 54 units are grouped into six 9-unit groups and each group of subproblems are solved together. Similar to traditional Lagrangian relaxation, we count an SLR iteration here as solving all subproblems (even though Lagrangian multipliers are updated six times). After termination, a near-optimal feasible UC solution is recovered. Results are summarized in the third column of Table III.

[6]The time required for generating models and updating multipliers is much longer than the CPU time of solving subproblems for SLR+B&C. This issue can be addressed by using more advanced optimization languages such as Julia instead of OPL.

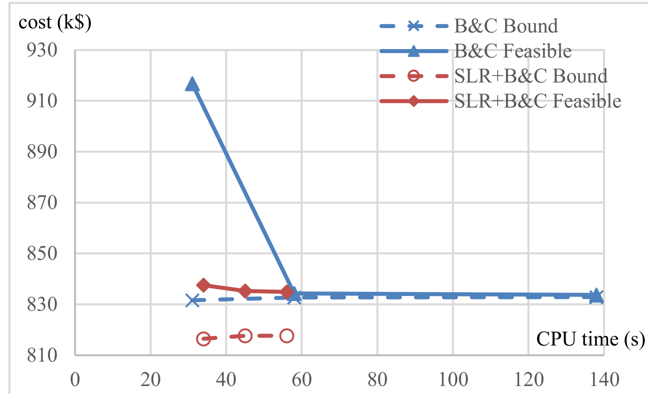

Fig. 6. Comparison between pure B&C and the SLR+B&C method for solving the interval CCUC model with the redundant constraint identification.

SLR+B&C finishes 20 iterations for the dual problem with the CPU time of 56 seconds. The total cost of the obtained feasible solution from SLR+B&C is $834.88k, very close to $834.26k of pure B&C. The simulation costs of both methods are also very close.

Fig. 6 further illustrates the computational performance of both methods for solving the CCUC model with redundant constraint identification. The pure B&C method obtains its first feasible solution of $916.83k at a 9.3% MIP gap after 31 seconds. However, it takes 58 seconds to reach the solution within the 0.5% MIP gap as in Table III, and takes 2 minutes and 18 seconds to obtain a solution of $833.72k at a 0.1% MIP gap. In contrast, the SLR+B&C method finishes 12 iterations for the dual problem after 34 seconds and obtains a feasible solution of $837.57k, only 0.46% higher than the $833.72k solution of B&C. This demonstrates that SLR+B&C is able to find a high-quality feasible solution in a shorter CPU time than B&C.

VI. CONCLUSION

This paper develops a novel interval optimization approach to manage both transmission contingencies and uncertain renewable generation in CCUC. Transmission contingencies are modeled by intervals for the first time, and its conservativeness is reduced. The resulting MILP problem is decomposed into unit-level subproblems so that SLR and B&C can be efficiently applied. The underlying idea of converting discrete events into continuous intervals can be used in other problems to capture multiple cases by one case.

ACKNOWLEDGMENT

The authors gratefully acknowledge the contributions of I. Lelic at ISO New England for insightful discussions and M. Bragin at the University of Connecticut for improving the SLR module.

REFERENCES

[1] Y. Yu, P. B. Luh, E. Litvinov, T. Zheng, J. Zhao, and F. Zhao, “Transmission contingency-constrained unit commitment with uncertain wind generation via interval optimization,” in *Proc. IEEE Power & Energy Soc. General Meeting*, Denver, CO, USA, Jul. 2015.
[2] A. J. Wood, B. F. Wollenberg, and G. B. Sheble, *Power Generation, Operation and Control*, 3rd ed. Hoboken, NJ, USA: Wiley, 2013.

[3] ISO New England, "ISO New England operating procedure no. 8 operating reserve and regulation," May 2015, [Online]. Available: http://www.iso-ne.com/rules_proceds/operating/isone/op8/op8_rto_final.pdf
[4] J. Zhu and K. Cheung, "Flexible simultaneous feasibility test in energy market," in *Proc. IEEE Power & Energy Soc. General Meeting*, Redmond, WA, USA, 2010.
[5] J. Wang, M. Shahidehpour, and Z. Li, "Contingency-constrained reserve requirements in joint energy and ancillary services auction," *IEEE Trans. Power Syst.*, vol. 24, no. 3, pp. 1457–1468, Aug. 2009.
[6] A. Street, F. Oliveira, and J. M. Arroyo, "Contingency-constrained unit commitment with security criterion: A robust optimization approach," *IEEE Trans. Power Syst.*, vol. 26, no. 3, pp. 1581–1590, Aug. 2011.
[7] Q. Wang, J-P. Watson, and Y. Guan, "Two-stage robust optimization for *N–k* contingency-constrained unit commitment," *IEEE Trans. Power Syst.*, vol. 28, no. 3, pp. 2366–2375, Aug. 2013.
[8] REN 21, "Renewables 2014 global status report," 2014. [Online]. Available: http://www.ren21.net/Portals/0/documents/Resources/GSR/2014/GSR2014_full%20report_low%20res.pdf
[9] D. Pozo and J. Contreras, "A chance-constrained unit commitment with an *n–K* security criterion and significant wind generation," *IEEE Trans. Power Syst.*, vol. 28, no. 3, pp. 2842–2851, Aug. 2013.
[10] A. Papavasiliou and S. Oren, "Multiarea stochastic unit commitment for high wind penetration in a transmission constrained network," *Oper. Res.*, vol. 61, no. 3, pp. 578–592, May/Jun. 2013.
[11] A. Moreira, A. Street, and J. M. Arroyo, "Energy and reserve scheduling under correlated nodal demand uncertainty: An adjustable robust optimization approach," *Electr. Power Energy Syst.*, vol. 72, pp. 91–98, Nov. 2015.
[12] Y. Yu, P. B. Luh, E. Litvinov, T. Zheng, J. Zhao, and F. Zhao, "Grid integration of distributed wind generation: Hybrid Markovian and interval unit commitment," *IEEE Trans. Smart Grid*, vol. 6, no. 6, pp. 3061–3072, Nov. 2015.
[13] W. Chinneck and K. Ramadan, "Linear programming with interval coefficients," *J. Oper. Res. Soc.*, vol. 51, no. 2, pp. 209–220, 2000.
[14] Y. Wang, Q. Xia, and C. Kang, "Unit commitment with volatile node injections by using interval optimization," *IEEE Trans. Power Syst.*, vol. 26, no. 3, pp. 1705–1713, Aug. 2011.
[15] Q. Zhai, X. Guan, J. Cheng, and H. Wu, "Fast identification of inactive security constraints in SCUC problems," *IEEE Trans. Power Syst.*, vol. 25, no. 4, pp. 1946–1954, Nov. 2010.
[16] M. A. Bragin, P. B. Luh, J. H. Yan, N. Yu, and G. A. Stern, "Convergence of the surrogate Lagrangian relaxation method," *J. Optimiz. Theory Appl.*, vol. 164, pp. 173–201, 2015.
[17] R. E. Bixby, M. Fenelon, Z. Gu, E. Rothberg, and R. Wunderling, "MIP: Theory and practice—Closing the gap," *Syst. Model. Optimiz.*, vol. 46, pp. 19–49, 2000.
[18] X. Sun and C. Fang, "Interval mixed-integer programming for daily unit commitment and dispatch incorporating wind power," in *Proc. Int. Conf. Power Syst. Technol.*, Hangzhou, China, Oct. 2010.
[19] L. Wu, M. Shahidehpour, and Z. Li, "Comparison of scenario-based and interval optimization approaches to stochastic SCUC," *IEEE Trans. Power Syst.*, vol. 27, no. 2, pp. 913–921, May 2012.
[20] Y. Dvorkin, H. Pandzic, M. A. Ortega-Vazquez, and D. S. Kirschen, "A hybrid stochastic/interval approach to transmission-constrained unit commitment," *IEEE Trans. Power Syst.*, vol. 30, no. 2, pp. 621–631, Mar. 2015.
[21] H. Pandžić, Y. Dvorkin, T. Qiu, Y. Wang, and D. S. Kirschen, "Toward cost-efficient and reliable unit commitment under uncertainty," *IEEE Trans. Power Syst.*, vol. 31, no. 2, pp. 970–982, Mar. 2016.
[22] X. Guan, P. B. Luh, H. Yan, and J. A. Amalfi, "An optimization-based method for unit commitment," *Int. J. Elect. Power Energy Syst.*, vol. 14, no. 1, pp. 9–17, 1992.
[23] D. Rajan and S. Takriti, "Minimum up/down polytopes of the unit commitment problem with start-up costs," IBM Res. Rep. RC23628, 2005.
[24] R. E. Moore, R. B. Kearfott and M. J. Cloud, *Introduction to Interval Analysis*. Philadelphia, PA, USA: SIAM, 2009.
[25] C. Zhao and Y. Guan, "Unified stochastic and robust unit commitment," *IEEE Trans. Power Syst.*, vol. 28, no. 3, pp. 3353–3361, Aug. 2013.
[26] E. Litvinov, T. Zheng, G. Rosenwald, and P. Shamsollahi, "Marginal loss modeling in LMP calculation," *IEEE Trans. Power Syst.*, vol. 19, no. 2, pp. 880–888, May 2004.
[27] A. Vaccaro, C. A. Canizares, and D. Villacci, "An affine arithmetic-based methodology for reliable power flow analysis in the presence of data uncertainty," *IEEE Trans. Power Syst.*, vol. 25, no. 2, pp. 624–632, May 2010.
[28] M. Pirnia, C. A. Cañizares, K. Bhattacharya, and A. Vaccaro, "A novel affine arithmetic method to solve optimal power flow problems with uncertainties," *IEEE Trans. Power Syst.*, vol. 29, no. 6, pp. 2775–2783, Nov. 2014.
[29] IEEE RTS Task Force of APM Subcommittee, "The IEEE reliability test system-1996," *IEEE Trans. Power Syst.*, vol. 14, no. 3, pp. 1010–1020, Aug. 1999.
[30] National Renewable Energy Laboratory, *Eastern Wind Dataset*. (2010). [Online]. Available: http://www.nrel.gov/electricity/transmission/eastern_wind_methodology.html
[31] F. Bouffard and F. D. Galiana, "Stochastic security for operations planning with significant wind power generation," *IEEE Trans. Power Syst.*, vol. 23, no. 2, pp. 306–316, May 2008.
[32] M. A. Ortega-Vazquez and D. S. Kirschen, "Estimating the spinning reserve requirements in systems with significant wind power generation penetration," *IEEE Trans. Power Syst.*, vol. 24, no. 1, pp. 114–124, Feb. 2009.
[33] L. Bird, J. Cochran, and X. Wang, "Wind and solar energy curtailment: Experience and practices in the United States," National Renewable Energy Laboratory, Golden, CO, USA, Tech. Rep. NREL/TP-6A20-60983, 2014.
[34] IEEE 118-bus system. (2014). [Online]. Available: http://motor.ece.iit.edu/data/

Yaowen Yu (S'12) received the B.S. degree in automation from Huazhong University of Science and Technology, Wuhan, China, in 2011, and the M.S. degree in electrical engineering from the University of Connecticut, Storrs, CT, USA, in 2014. He is currently working toward the Ph.D. degree at the University of Connecticut. His research interests include power system optimization, grid integration of renewable energy, and economics of electricity markets.

Peter B. Luh (S'77–M'80–SM'91–F'95) received the B.S. degree from National Taiwan University, the M.S. degree from M.I.T., and the Ph.D. degree from Harvard University. He has been with the University of Connecticut since 1980, and is the SNET Professor of Communications & Information Technologies. His research interests include smart power systems–smart grid, design of auction methods for electricity markets, effective renewable (wind and solar) integration to the grid, electricity load and price forecasting with demand response, and micro grid. He was the Vice-President of Publication Activities for the IEEE Robotics and Automation Society.

Eugene Litvinov (SM'06–F'12) received the B.S. and M.S. degrees from the Technical University, Kiev, Ukraine, and the Ph.D. degree from Urals Polytechnic Institute, Sverdlovsk, Russia. He is currently the Chief Technologist at ISO New England, Holyoke, MA, USA. His research interests include power system market-clearing models, system security, computer applications to power systems, and information technology.

Tongxin Zheng (SM'08) received the B.S. degree in electrical engineering from North China Institute of Electric Power, Baoding, China, in 1993, the M.S. degree in electrical engineering from Tsinghua University, Beijing, China, in 1996, and the Ph.D. degree in electrical engineering from Clemson University, Clemson, SC, USA, in 1999. He is currently a Technical Manager at ISO New England. His main research interests include power system optimization and electricity market design.

Jinye Zhao (M'11) received the B.S. degree from East China Normal University, Shanghai, China, in 2002, the M.S. degree in mathematics from National University of Singapore, Singapore, in 2004, and the M.S. degree in operations research and statistics and the Ph.D. degree in mathematics from Rensselaer Polytechnic Institute, Troy, NY, USA, in 2007. She is currently a Lead Analyst at ISO New England, Holyoke, MA, USA. Her main interests include game theory, mathematical programming, and electricity market modeling.

Feng Zhao (M'08) received the B.S. degree in automatic control from Shanghai JiaoTong University, Shanghai, China, in 1998, the M.S. degree in control theory and control engineering from Tsinghua University, Beijing, China, in 2001, and the Ph.D. degree in electrical engineering from the University of Connecticut, Storrs, CT, USA, in 2008. He is currently a Lead Analyst at ISO New England, Holyoke, MA, USA. His research interests include mathematical optimization, power system planning and operations, and economics of electricity markets.

Dane A. Schiro (M'14) received the B.S. degree in environmental engineering from the Johns Hopkins University, Baltimore, MD, USA, and the Ph.D. degree in industrial engineering from the University of Illinois, Urbana, IL, USA. He is currently an Analyst at ISO New England, Holyoke, MA, USA. His research interests include the intersection of optimization theory, economics, and operations.